

Revisiting the Strong Stretching Theory for pH-Responsive Polyelectrolyte Brushes: Effects of Consideration of Excluded Volume Interactions and an Expanded Form of the Mass Action Law

Harnoor Singh Sachar, Vishal Sankar Sivasankar, and Siddhartha Das

Department of Mechanical Engineering, University of Maryland, College Park, MD-20742, USA

(Dated: November 15, 2018)

Abstract: In this paper, we develop a theory to account for the effect of the excluded volume (EV) interactions in the Strong Stretching Theory (SST) based description of the pH-responsive polyelectrolyte (PE) brushes. The existing studies have considered the PE brushes to be present in a θ -solvent and hence have neglected the EV interactions; however, such a consideration cannot describe the situations where the pH-responsive brushes are in a “good” solvent. Secondly, we consider a more expanded form of the mass action law, governing the pH-dependent ionization of the PE molecules, in the SST description of the PE brushes. This expanded form of the mass action law considers different values of γa^3 (γ is the density of the chargeable sites on the PE molecule and a is the PE Kuhn length) and therefore is an improvement over the existing SST models of PE brushes as well as other theories involving pH-responsive PE molecules that always consider $\gamma a^3 = 1$. Our results demonstrate that the EV effects enhance the brush height by inducing additional PE inter-segmental repulsion. Similarly, the consideration of the expanded form of the mass action law would lead to a reduced (enhanced) brush height for $\gamma a^3 < 1$ ($\gamma a^3 > 1$). We also quantify the variables such as the monomer density distribution, distribution of the ends of the PE brush, and the EDL electrostatic potential and explain their differences with respect to those obtained with no EV interactions or $\gamma a^3 = 1$.

I. INTRODUCTION

Grafting charged, polyelectrolyte (PE) brushes on solid-liquid interfaces have proven to be an excellent way of functionalizing such interfaces for applications such as nanofluidic ion and biosensing [1–5], fabrication of nanofluidic diodes [6, 7], current rectifiers [8], and nano-actuators [9], designing surfaces of desired wettability [10], engineering nanoparticles for targeted drug delivery [11], oil recovery [12], and many more. The key to several of these applications is the responsiveness of these brushes to environmental cues (e.g., a change in pH or a change in salt concentration) – as a response to these cues, the PE brushes undergo a change in some of its properties (e.g., configuration, height, etc.) thereby enabling most of these above applications. pH-responsive (or annealed) PE brushes refer to brushes whose ionization and hence the charging depends on the local pH [13–17]. For example, poly(meth)acrylic brush is an example of a pH-responsive anionic brush. On the other hand, there are brushes (also known as quenched brushes) whose degree of ionization and hence the charging is independent of pH (e.g., partially sulfonated polystyrene brushes). The purpose of this paper is to provide a detailed thermodynamic self-consistent theoretical model for quantifying such pH-responsive PE brushes.

PE brushes have been modelled extensively. For example, there have been significant efforts aimed at developing scaling laws by balancing the different energies (elastic, electrostatic, and excluded volume) and yielded the brush height as scaled functions of variables such as the grafting density and charge density of the brushes, number of monomers, and the concentration of the added salt [18–25]. Subsequently, a more involved calculation procedure was also attempted where the electrostatics of the induced electric double layer (EDL) was described using the Poisson-Boltzmann (PB) equation [15, 17, 26–31]. Such studies varied in complexity and rigour depending on the manner in which the monomer interactions were described – there have been several approaches ranging from the use of simple Alexander-de-Gennes model [27–30] to a more involved parabolic model [26, 31] for the brushes. The most complete analytically tractable approach till date, however, has been proposed in a series of seminal papers that employed the Strong Stretching Theory (SST) to describe the PE brushes while the resulting EDL electrostatics was described by the classical PB equation [13, 32–35].

The same self-consistent SST and the PB equation have also been employed to study the configuration of the pH-responsive PE brushes [13]. This study is the state-of-the-art in the SST calculation of the pH-responsive PE brushes. However, this paper considers the PE brushes to be in a θ -solvent and hence neglects all the possible excluded volume (EV) interactions. On the other hand, a vast number of experimental studies involving pH-responsive PE brushes invariably consider the solvent to be a “good” solvent (i.e., a solvent that makes the considerations of the EV interactions between the segments of the PE molecule mandatory) with respect to the PE brush [36–43]. Obviously, for such problems, the theory of Ref.[13] will be inadequate. In order to fill this void, in this paper, we modify the SST for the pH-responsive PE brushes by accounting for the EV interactions between the PE brush segments. Therefore, this study is the first study for the SST of the pH-responsive PE brushes accounting for the effect of the EV

interactions. EV interactions have been considered for other theoretical calculations of the PE brushes [44–46], but not in this SST framework used to quantify the behavior of the pH-responsive PE brushes. As a second improvement to the SST model of the pH-responsive PE brushes, we consider a more expanded form of the mass action law for the pH-dependent ionization of the PE molecules valid for all values of γa^3 (γ is the density of the chargeable sites on the PE molecule and a is the PE Kuhn length) and study the effect of this more expanded form of the mass action law in the SST calculations of PE brushes. Both Ref. [13] as well as other papers describing the pH-responsive PE molecules (not necessarily PE “brushes”) [47–51] have considered only a special form of the mass action law where $\gamma a^3 = 1$. Our calculations, therefore, ensure a more generic description of the pH-responsive PE brushes within the general ambit of the SST model.

Our results demonstrate distinct contributions of the EV interactions and the expanded form of the mass action law in the SST description of the PE brushes. Consideration of the EV interactions imply consideration of additional inter-segmental repulsion for a particular PE brush molecule. Accordingly, the EV effect enhances the brush height. This enhancement is most magnified for large salt concentration (which leads to an enhanced screening of the PE brush charges) and small pH_∞ (i.e., a large bulk H^+ ion concentration that weakens the ionization of the brushes). On the other hand, consideration of the generic mass action law implies that one witnesses a decrease (increase) of the PE brush height for $\gamma a^3 < 1$ ($\gamma a^3 > 1$) owing to a reduced (enhanced) charge density of the PE brushes causing a reduced (enhanced) counterion-induced brush swelling [52–54]. We complete the description of the problem by accounting for the effects of the EV interactions and the expanded form of the mass action law in dictating the monomer density distribution, distribution of the end location of the PE brushes, and the EDL electrostatics. In summary, our paper establishes the theory for a much more generic SST-based description of the pH-responsive PE brushes and the resultant EDL electrostatics.

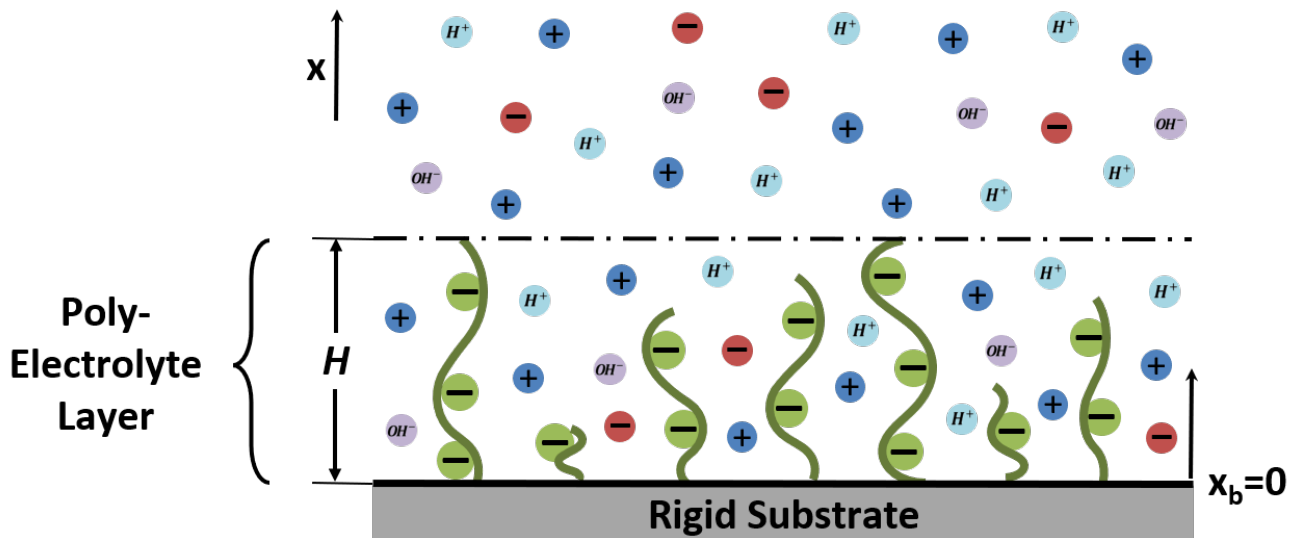


FIG. 1: Schematic showing the pH-responsive PE brush layer.

II. SELF-CONSISTENT FIELD APPROACH

A. Free Energy Equations

We consider a rigid, impenetrable substrate grafted with pH-responsive, weakly poly-acidic (anionic) PE brushes immersed in an electrolyte solution (see Fig. 1). The separation between adjacent grafted PE molecules ℓ is assumed to be small enough such that the system attains a brush like configuration. Here we would discuss the free energies that dictate the brush equilibrium in a self-consistent field approach. These equations have already been discussed by several previous papers [13, 32, 44]; we repeat them here for the sake of continuity.

The net free energy functional (F) of a given PE molecule can be expressed as:

$$\frac{F}{k_B T} = \frac{F_{els}}{k_B T} + \frac{F_{EV}}{k_B T} + \frac{F_{elec}}{k_B T} + \frac{F_{EDL}}{k_B T} + \frac{F_{ion}}{k_B T}, \quad (1)$$

where F_{els} , F_{EV} , F_{elec} , F_{EDL} and F_{ion} are the elastic (entropic), excluded volume, electrostatic, electric double layer and ionization contributions to the free energy (per PE molecule) respectively.

In this model, the equilibrium brush height H (to be determined self-consistently later) refers to the maximum distance of the monomers of the PE brush from the substrate. In order to express the free energy, the system is divided into two regions: region 1 ($0 \leq x \leq H$) forms the interior of the brush and comprises of all the PE chains whereas the region 2 ($H \leq x \leq \infty$) lies exterior to the brush. We consider the case where the electrostatic repulsion between the charged monomers is large enough to ensure that the brush is in a strongly stretched configuration. Therefore this free energy description is the same as the *Strong Stretching Theory* description of the PE brushes.

Following the notation of Zhulina et al. [44], we write:

$$\frac{F_{els}}{k_B T} = \frac{3}{2pa^2} \int_0^H g(x') dx' \int_0^{x'} E(x, x') dx, \quad (2)$$

$$\frac{F_{EV}}{k_B T} = \frac{\sigma}{a^3} \int_0^H f_{conc}[\phi(x)] dx, \quad (3)$$

where p is the chain rigidity, a is the Kuhn length, and $\sigma \sim \ell^2$ is the grafted area per chain. Also, $E(x, x') = \frac{dx}{dn}$ is the local stretching at a distance x from the surface for a chain whose end is located at a distance of x' . Furthermore, $g(x')$ is the normalized chain end distribution function, such that

$$\int_0^H g(x') dx' = 1. \quad (4)$$

Finally, $\phi(x)$ is the dimensionless monomer distribution profile of a given PE chain and $f_{conc}[\phi(x)]$ is the non-dimensionalized per unit-volume free energy for the excluded volume interactions.

Following [17], $F_{elec} + F_{EDL}$ can be expressed as:

$$\begin{aligned} \frac{F_{elec}}{k_B T} + \frac{F_{EDL}}{k_B T} &= \frac{\sigma}{k_B T} \int_0^\infty \left[-\frac{\epsilon_0 \epsilon_r}{2} \left| \frac{d\psi}{dx} \right|^2 + e\psi(n_+ - n_- + n_{H^+} - n_{OH^-}) \right] dx - \frac{\sigma}{k_B T} \int_0^H [e\psi n_{A^-} \phi] dx + \\ &\sigma \int_0^\infty \left[n_+ \left(\ln \left(\frac{n_+}{n_{+, \infty}} \right) - 1 \right) + n_- \left(\ln \left(\frac{n_-}{n_{-, \infty}} \right) - 1 \right) + n_{H^+} \left(\ln \left(\frac{n_{H^+}}{n_{H^+, \infty}} \right) - 1 \right) \right. \\ &\left. + n_{OH^-} \left(\ln \left(\frac{n_{OH^-}}{n_{OH^-, \infty}} \right) - 1 \right) + (n_{+, \infty} + n_{-, \infty} + n_{H^+, \infty} + n_{OH^-, \infty}) \right] dx \end{aligned} \quad (5)$$

where ψ is the electrostatic potential, n_i is the number density of the ion i [where $i = \pm, H^+, OH^-$], $n_{i, \infty}$ is the bulk number density of the ion i , n_{A^-} is the local number density of the A^- ion, e is the electronic charge, $k_B T$ is the thermal energy, ϵ_0 is the permittivity of free space, and ϵ_r is the relative permittivity of the solution.

The PE brush ionizes via dissociation of an acid HA producing H^+ and A^- ions. n_{A^-} is a function of the hydrogen ion concentration (n_{H^+}) as given by the expanded form of the mass action law (see the derivation later).

Following [13], F_{ion} can be expressed as:

$$\begin{aligned} \frac{F_{ion}}{k_B T} &= \frac{\sigma}{a^3} \int_0^H \phi \left[\left(1 - \frac{n_{A^-}}{\gamma} \right) \ln \left(1 - \frac{n_{A^-}}{\gamma} \right) + \frac{n_{A^-}}{\gamma} \ln \left(\frac{n_{A^-}}{\gamma} \right) + \frac{n_{A^-}}{\gamma} \left(\frac{\mu_{H^+}^0 + \mu_{A^-}^0 - \mu_{AH}^0}{k_B T} + \ln(c_{H^+, \infty}) \right) \right] dx \\ \implies \frac{F_{ion}}{k_B T} &= \frac{\sigma}{a^3} \int_0^H \phi \left[\left(1 - \frac{n_{A^-}}{\gamma} \right) \ln \left(1 - \frac{n_{A^-}}{\gamma} \right) + \frac{n_{A^-}}{\gamma} \ln \left(\frac{n_{A^-}}{\gamma} \right) + \frac{n_{A^-}}{\gamma} \ln \left(\frac{n_{H^+, \infty}}{K'_a} \right) \right] dx \end{aligned} \quad (6)$$

where $K'_a = 10^3 N_A K_a$, N_A is the Avogadro number and K_a is the ionization constant of the reaction $HA \rightarrow H^+ + A^-$. Also $K_a = \exp\left(-\frac{\mu_{H^+}^0 + \mu_{A^-}^0 - \mu_{AH}^0}{k_B T}\right)$, where μ_i^0 represents the standard chemical potential of species i . $n_{H^+, \infty} = 10^3 N_A c_{H^+, \infty}$ and γ ($1/m^3$) is the maximum density of polyelectrolyte chargeable sites (PCS).

Substituting eqs.(2,3,5,6) in eq.(1), F can be written as:

$$\begin{aligned} \frac{F}{k_B T} = & \frac{3}{2pa^2} \int_0^H g(x') dx' \int_0^{x'} E(x, x') dx + \frac{\sigma}{a^3} \int_0^H f_{conc}[\phi(x)] dx + \frac{\sigma}{k_B T} \int_0^\infty \left[-\frac{\epsilon_0 \epsilon_r}{2} \left| \frac{d\psi}{dx} \right|^2 \right. \\ & \left. + e\psi(n_+ - n_- + n_{H^+} - n_{OH^-}) \right] dx - \frac{\sigma}{k_B T} \int_0^H \left[e\psi n_{A^-} \phi \right] dx + \sigma \int_0^\infty \left[n_+ \left(\ln\left(\frac{n_+}{n_{+, \infty}}\right) - 1 \right) \right. \\ & \left. + n_- \left(\ln\left(\frac{n_-}{n_{-, \infty}}\right) - 1 \right) + n_{H^+} \left(\ln\left(\frac{n_{H^+}}{n_{H^+, \infty}}\right) - 1 \right) + n_{OH^-} \left(\ln\left(\frac{n_{OH^-}}{n_{OH^-, \infty}}\right) - 1 \right) \right. \\ & \left. + (n_{+, \infty} + n_{-, \infty} + n_{H^+, \infty} + n_{OH^-, \infty}) \right] dx \\ & + \frac{\sigma}{a^3} \int_0^H \phi \left[\left(1 - \frac{n_{A^-}}{\gamma} \right) \ln\left(1 - \frac{n_{A^-}}{\gamma} \right) + \frac{n_{A^-}}{\gamma} \ln\left(\frac{n_{A^-}}{\gamma} \right) + \frac{n_{A^-}}{\gamma} \ln\left(\frac{n_{H^+, \infty}}{K'_a} \right) \right] dx \end{aligned} \quad (7)$$

This energy needs to be minimized in presence of the following conditions (constraints):

$$N = \int_0^{x'} \frac{dx}{E(x, x')}, \quad (8)$$

$$N = \frac{\sigma}{a^3} \int_0^H \phi(x) dx, \quad (9)$$

where N is the number of monomers per chain.

Also $\phi(x)$ is related to the functions g and E as:

$$\phi(x) = \frac{a^3}{\sigma} \int_x^H \frac{g(x') dx'}{E(x, x')}. \quad (10)$$

Accounting for the constraints, the elastic component of free energy can be expressed in terms of Lagrange multipliers [λ_1 and $\lambda_2(x')$] as:

$$\frac{F'_{els}}{k_B T} = \frac{3}{2pa^2} \int_0^H g(x') dx' \int_0^{x'} E(x, x') dx + \lambda_1 \left[\frac{\sigma}{a^3} \int_0^H \phi(x) dx - N \right] + \int_0^H \lambda_2(x') dx' \left[\int_0^{x'} \frac{dx}{E(x, x')} - N \right]. \quad (11)$$

Therefore, the net free energy (F') accounting for all the constraints is:

$$\frac{F'}{k_B T} = \frac{F'_{els}}{k_B T} + \frac{F_{EV}}{k_B T} + \frac{F_{elec}}{k_B T} + \frac{F_{EDL}}{k_B T} + \frac{F_{ion}}{k_B T} \quad (12)$$

B. Variational Formalism

We would like to obtain the governing equations dictating the problem by carrying a variational minimization of eq.(12). Variation of eq.(12), i.e.,

$$\frac{\delta F'}{k_B T} = \frac{\delta F'_{els}}{k_B T} + \frac{\delta F_{EV}}{k_B T} + \frac{\delta F_{elec}}{k_B T} + \frac{\delta F_{EDL}}{k_B T} + \frac{\delta F_{ion}}{k_B T} = 0. \quad (13)$$

The condition $\delta F'=0$ leads to the following equations (see appendix A for the detailed derivation), which stem from the fact that $\delta E(x, x') \neq 0$, $\delta g(x') \neq 0$, $\delta \psi \neq 0$, $\delta n_{A^-} \neq 0$, $\delta n_{\pm} \neq 0$, $\delta n_{H^+} \neq 0$, $\delta n_{OH^-} \neq 0$:

$$\begin{aligned} & \frac{3g(x')}{2a^2} - \frac{\lambda_2(x')}{E^2(x, x')} - \left(\frac{\delta f_{conc}}{\delta \phi} + \lambda_1 - \frac{ea^3\psi}{k_B T} n_{A^-} + \left(1 - \frac{n_{A^-}}{\gamma}\right) \ln\left(1 - \frac{n_{A^-}}{\gamma}\right) \right. \\ & \left. + \frac{n_{A^-}}{\gamma} \ln\left(\frac{n_{A^-}}{\gamma}\right) + \frac{n_{A^-}}{\gamma} \ln\left(\frac{n_{H^+, \infty}}{K'_a}\right) \right) \frac{g(x')}{E^2(x, x')} = 0, \end{aligned} \quad (14)$$

$$\begin{aligned} & \int_0^{x'} \left[\frac{3E(x, x')}{2a^2} + \left(\frac{\delta f_{conc}}{\delta \phi} + \lambda_1 - \frac{ea^3\psi}{k_B T} n_{A^-} + \left(1 - \frac{n_{A^-}}{\gamma}\right) \ln\left(1 - \frac{n_{A^-}}{\gamma}\right) + \frac{n_{A^-}}{\gamma} \ln\left(\frac{n_{A^-}}{\gamma}\right) \right. \right. \\ & \left. \left. + \frac{n_{A^-}}{\gamma} \ln\left(\frac{n_{H^+, \infty}}{K'_a}\right) \right) \frac{1}{E(x, x')} \right] dx = 0, \end{aligned} \quad (15)$$

$$\begin{aligned} & -\gamma a^3 \frac{e\psi}{k_B T} - \ln\left(1 - \frac{n_{A^-}}{\gamma}\right) + \ln\left(\frac{n_{A^-}}{\gamma}\right) + \ln\left(\frac{n_{H^+, \infty}}{K'_a}\right) = 0 \\ & \implies n_{A^-} = \frac{K'_a \gamma}{K'_a + n_{H^+, \infty} \exp\left(-\gamma a^3 \frac{e\psi}{k_B T}\right)} \end{aligned} \quad (16)$$

$$\begin{aligned} \epsilon_0 \epsilon_r \left(\frac{d^2 \psi}{dx^2} \right) + e(n_+ - n_- + n_{H^+} - n_{OH^-} - n_{A^-} \phi) &= 0 \quad (0 \leq x \leq H) \\ \epsilon_0 \epsilon_r \left(\frac{d^2 \psi}{dx^2} \right) + e(n_+ - n_- + n_{H^+} - n_{OH^-}) &= 0 \quad (H \leq x \leq \infty), \end{aligned} \quad (17)$$

$$n_{\pm} = n_{\pm, \infty} \exp\left(\mp \frac{e\psi}{k_B T}\right), \quad (18)$$

$$n_{H^+} = n_{H^+, \infty} \exp\left(-\frac{e\psi}{k_B T}\right), \quad (19)$$

$$n_{OH^-} = n_{OH^-, \infty} \exp\left(\frac{e\psi}{k_B T}\right), \quad (20)$$

Eq. (16) is the expanded form of the mass action law that we shall use here. On the other hand, all the existing studies have invariably considered $\gamma = 1/a^3$ and accordingly, have considered a form of the mass action law expressed as [13]:

$$n_{A^-} = \frac{K'_a \gamma}{K'_a + n_{H^+, \infty} \exp\left(-\frac{e\psi}{k_B T}\right)}. \quad (21)$$

This study, therefore, will reveal for the first time the effect of consideration of the mass action law in dictating the strong stretching behavior of the pH-responsive PE brushes.

Now, from eq.(14), we get:

$$E(x, x') = \sqrt{U_1(x') - U_2(x)}, \quad (22)$$

where

$$U_1(x') = \frac{2a^2}{3} \frac{\lambda_2(x')}{g(x')}, \quad (23)$$

$$U_2(x) = \frac{2a^2}{3} \left(-\frac{\delta f_{conc}}{\delta \phi} - \lambda_1 + \frac{ea^3\psi}{k_B T} n_{A^-} - \left(1 - \frac{n_{A^-}}{\gamma}\right) \ln\left(1 - \frac{n_{A^-}}{\gamma}\right) - \frac{n_{A^-}}{\gamma} \ln\left(\frac{n_{A^-}}{\gamma}\right) - \frac{n_{A^-}}{\gamma} \ln\left(\frac{n_{H^+, \infty}}{K'_a}\right) \right). \quad (24)$$

Since there is no extension at the brush ends, $E(x, x) = 0$. Therefore, $U_1(x) = U_2(x) = U(x)$. Hence,

$$E(x, x') = \sqrt{U(x') - U(x)}. \quad (25)$$

The normalization condition of eq.(8) serves as an integral equation for $U(x')$. One can check that this integral equation is satisfied if:

$$U(x) = \frac{\pi^2 x^2}{4N^2} \quad (26)$$

Consequently,

$$E(x, x') = \frac{\pi}{2N} \sqrt{x'^2 - x^2}. \quad (27)$$

Now we can re-write eq.(15) as:

$$\int_0^{x'} \left[E(x, x') - \frac{U(x)}{E(x, x')} \right] dx = 0. \quad (28)$$

Eq.(28) is equally satisfied with these stated forms of $U(x)$ and $E(x, x')$. To obtain $\phi(x)$ we can employ eq.(24), but prior to that we would need the functional dependence of f on ϕ . Considering the virial expansion for the non-dimensionalised per-unit volume free energy of volume interactions, we can write [44]:

$$f_{conc}[\phi(x)] \approx \nu\phi^2 + \omega\phi^3 + \dots, \quad (29)$$

where ν and ω are the virial coefficients.

Considering the first two terms of the expansion of $f_{conc}[\phi(x)]$, we can use eq. (24) to obtain $\phi(x)$ in terms of $\psi(x)$ by solving a quadratic equation:

$$\begin{aligned} \phi(x) = \frac{\nu}{3\omega} \left[\right. & \left. \left\{ 1 + \kappa^2 \left(\lambda - x^2 + \beta \frac{K'_a \gamma}{K'_a + n_{H^+, \infty} \exp(-\gamma a^3 \frac{e\psi}{k_B T})} \right) \psi \right. \right. \\ & - \rho \left(1 - \frac{K'_a}{K'_a + n_{H^+, \infty} \exp(-\gamma a^3 \frac{e\psi}{k_B T})} \right) \ln \left(1 - \frac{K'_a}{K'_a + n_{H^+, \infty} \exp(-\gamma a^3 \frac{e\psi}{k_B T})} \right) \\ & - \rho \frac{K'_a}{K'_a + n_{H^+, \infty} \exp(-\gamma a^3 \frac{e\psi}{k_B T})} \ln \left(\frac{K'_a}{K'_a + n_{H^+, \infty} \exp(-\gamma a^3 \frac{e\psi}{k_B T})} \right) \\ & \left. \left. - \rho \frac{K'_a}{K'_a + n_{H^+, \infty} \exp(-\gamma a^3 \frac{e\psi}{k_B T})} \ln \left(\frac{n_{H^+, \infty}}{K'_a} \right) \right\}^{1/2} - 1 \right], \quad (30) \end{aligned}$$

where,

$$\kappa^2 = \frac{9\pi^2 \omega}{8N^2 a^2 \nu^2}, \quad (31)$$

$$\rho = \frac{8a^2 N^2}{3\pi^2}, \quad (32)$$

$$\lambda = -\lambda_1 \rho = -\lambda_1 \frac{8a^2 N^2}{3\pi^2}, \quad (33)$$

$$\beta = \frac{8N^2 ea^5}{3\pi^2 k_B T}. \quad (34)$$

Using eqs. (16), (18), (19), (20) and (30), we can re-write the equations governing ψ as:

$$\begin{aligned} \epsilon_0 \epsilon_r \left(\frac{d^2 \psi}{dx^2} \right) + e \left(n_{+, \infty} \exp \left(- \frac{e\psi}{k_B T} \right) - n_{-, \infty} \exp \left(\frac{e\psi}{k_B T} \right) + n_{H^+, \infty} \exp \left(- \frac{e\psi}{k_B T} \right) - n_{OH^-, \infty} \exp \left(\frac{e\psi}{k_B T} \right) \right. \\ - \frac{K'_a \gamma}{K'_a + n_{H^+, \infty} \exp \left(- \gamma a^3 \frac{e\psi}{k_B T} \right)} \frac{\nu}{3\omega} \left[\left. 1 + \kappa^2 \left(\lambda - x^2 + \beta \frac{K'_a \gamma}{K'_a + n_{H^+, \infty} \exp \left(- \gamma a^3 \frac{e\psi}{k_B T} \right)} \psi \right. \right. \right. \\ \left. \left. - \rho \left(1 - \frac{K'_a}{K'_a + n_{H^+, \infty} \exp \left(- \gamma a^3 \frac{e\psi}{k_B T} \right)} \right) \ln \left(1 - \frac{K'_a}{K'_a + n_{H^+, \infty} \exp \left(- \gamma a^3 \frac{e\psi}{k_B T} \right)} \right) \right. \right. \\ \left. \left. - \rho \frac{K'_a}{K'_a + n_{H^+, \infty} \exp \left(- \gamma a^3 \frac{e\psi}{k_B T} \right)} \ln \left(\frac{K'_a}{K'_a + n_{H^+, \infty} \exp \left(- \gamma a^3 \frac{e\psi}{k_B T} \right)} \right) \right. \right. \\ \left. \left. - \rho \frac{K'_a}{K'_a + n_{H^+, \infty} \exp \left(- \gamma a^3 \frac{e\psi}{k_B T} \right)} \ln \left(\frac{n_{H^+, \infty}}{K'_a} \right) \right) \right]^{1/2} - 1 \Bigg) = 0 \quad (0 \leq x \leq H), \end{aligned}$$

$$\epsilon_0 \epsilon_r \left(\frac{d^2 \psi}{dx^2} \right) + e \left(n_{+, \infty} \exp \left(- \frac{e\psi}{k_B T} \right) - n_{-, \infty} \exp \left(\frac{e\psi}{k_B T} \right) + n_{H^+, \infty} \exp \left(- \frac{e\psi}{k_B T} \right) - n_{OH^-, \infty} \exp \left(\frac{e\psi}{k_B T} \right) \right) = 0 \quad (H \leq x \leq \infty). \quad (35)$$

Eqs.(29,35) establish that the equations governing the monomer distribution and the EDL electrostatic potential involve the parameters (ν, ω) dictating the excluded volume interactions enabling for the first time the inclusion of the excluded volume interactions in the SST description of the pH-responsive PE brushes. As has been already discussed, the state of the art SST invariably neglect the EV effects, i.e., consider the brushes to be always in a θ -solvent, which might be scenario far from reality.

The boundary conditions for solving ψ are:

$$(\psi)_{x=H^-} = (\psi)_{x=H^+}, \quad \left(\frac{d\psi}{dx} \right)_{x=H^-} = \left(\frac{d\psi}{dx} \right)_{x=H^+}, \quad \left(\frac{d\psi}{dx} \right)_{x=0} = 0, \quad (\psi)_{x \rightarrow \infty} = 0. \quad (36)$$

From eq.(35) we can solve for ψ for a given H, provided we know λ . λ is obtained by using the normalization condition provided by eq.(9). In other words, we shall need to solve eqs.(35,9) simultaneously, as well as employ eq.(30) to obtain ϕ , ψ and λ . Now that we have $\phi(x)$, $\psi(x)$, $n_{A^-}(\psi)$, $n_{\pm} = n_{\pm}(\psi)$, $n_{H^+} = n_{H^+}(\psi)$, $n_{OH^-} = n_{OH^-}(\psi)$ we can obtain the net unbalanced charge (q_{net}) in the system as a function of H.

$$q_{net} = e\sigma \int_0^\infty (n_+ - n_- + n_{H^+} - n_{OH^-} - \phi n_{A^-}) dx \quad (37)$$

In order to obtain the equilibrium brush height H, which is H_0 , we will obtain the resulting equation (in terms of H_0) by writing:

$$(q_{net})_{H=H_0} = 0 \quad (38)$$

Finally, we can obtain $g(x)$ by inverting the integral equation provided by eq.(10) in presence of eq.(27) as:

$$g(x) = \frac{x\sigma}{Na^3} \left[\frac{\phi(H)}{\sqrt{H^2 - x^2}} - \int_x^H \frac{d\phi(x')}{dx'} \frac{dx'}{\sqrt{x'^2 - x^2}} \right] \quad (39)$$

III. RESULTS

A. Effects of consideration of excluded volume interactions

The state-of-the-art SST calculations for describing the pH-responsive PE brushes neglect the EV interactions, i.e., assume that the brushes are in a θ -solvent. However, a more generic consideration must account for the possibilities

that the brushes might be present in a “good” solvent, so that there is a finite EV interactions between brush segments. In the present case, we account for such a generic consideration and consider varying extent of the “goodness” of the solvent, quantified by the different values of the parameters ν and ω . For simplicity, we define a given solvent using different values of ν and a given value of ω . Obviously, the results corresponding to $\nu = 0, \omega = 0$ represent the case of the θ -solvent [13].

In Fig. 2(a), we elucidate the variation of the brush height as a function of the extent of the EV interactions (quantified by different values of ν and a given value of ω). Larger EV interactions, characterized by larger values of ν and ω , would enforce a larger separation between the segments of the PE brushes, and accordingly lead to a larger value of the brush height [see Fig. 2(a)]. Of course, the case of $\nu = 0, \omega = 0$ is the case where the EV interactions have been ignored. We have checked that the results $\nu = 0, \omega = 0$ from our calculations is exactly identical to that obtained by Zhulina and Borisov [13], who consider a θ -solvent (no EV interactions). An increase in the salt concentration reduces the brush height for all the values of ν and ω . A larger salt concentration leads to a smaller EDL thickness and hence there is a screening of the electrostatic repulsion over much shorter distance, eventually reducing the brush height with the salt concentration, as has been revealed previously [24, 27]. On the other hand, a larger pH_∞ or a smaller value of bulk H^+ ion concentration leads to a stronger ionization reaction (i.e., there is an enhancement of the reaction that produces H^+ ions) and hence a larger charge of the PE brushes ensuring a larger counterion-induced osmotic swelling [52–54] causing to a larger brush height for all values of ν and ω . The relative contribution of the EV interactions in altering the brush height (quantified by the ratio $\Delta H_0/H_0$) has been probed in Fig. 2(b). We find that the maximum percentage difference occurs for the case of larger salt concentration and smaller pH_∞ . Larger salt concentration (or a smaller EDL thickness) and smaller pH_∞ (or a larger H^+ ion concentration leading to a weakened PE ionization) ensure weakened charging of the PE brushes and hence weakened counterion-induced osmotic swelling of the brushes. Under such circumstances, therefore, the relative contribution of the EV-interactions (and the resulting inter segment repulsions) in enhancing the brush height becomes more important as reflected by the larger values of $\Delta H_0/H_0$ for such concentration and pH_∞ values. This is the first key finding of the paper: the EV interactions, neglected in all previous studies of SST for pH-responsive PE brushes [13], become extremely important in dictating the brush height for large salt concentration and small pH_∞ values.

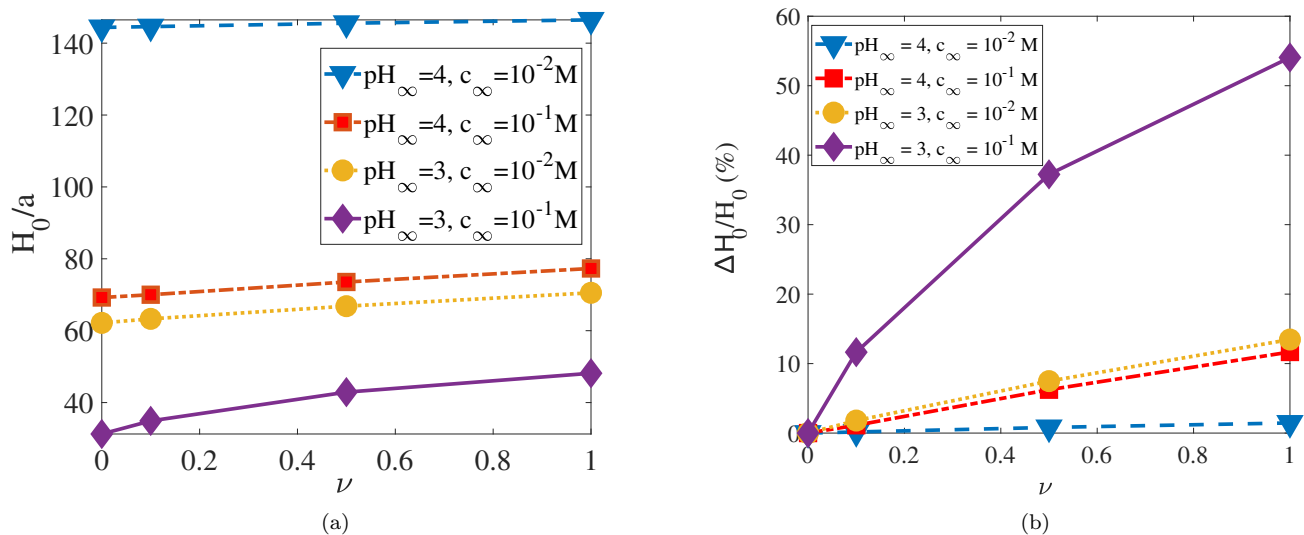


FIG. 2: Variation of (a) non-dimensional equilibrium brush height H_0/a (a is the PE Kuhn length) and (b) percentage increase in equilibrium brush height $\Delta H_0/H_0$ (where $\Delta H_0 = H_0 - H_{0,\nu=0,\omega=0}$) with the first virial coefficient ν for different pH_∞ and c_∞ values. The case of Ref.[13] is the one where $\nu = 0, \omega = 0$ – we recover exactly the results of Ref.[13] when $\nu = 0, \omega = 0$. Other parameters for this figure are $\omega = 0.1, pK_a = 3.5, a = 1 \text{ nm}, \gamma = 1/a^3$ (1 PCS per kuhn monomer), $N = 662, \ell = 40 \text{ nm}, k_B = 1.38 \times 10^{-23} \text{ J/K}, T = 298 \text{ K}, e = 1.6 \times 10^{-19} \text{ C}, \epsilon_0 = 8.854 \times 10^{-12} \text{ F/m}, \epsilon_r = 79.8, pK_w = 14, pOH_\infty = pK_w - pH_\infty, c_{+, \infty} = c_\infty, c_{H^+, \infty} = 10^{-pH_\infty}, c_{OH^-, \infty} = 10^{-pOH_\infty}, c_{-, \infty} = c_\infty + c_{H^+, \infty} - c_{OH^-, \infty}$.

Fig. 3 provides the variation of the monomer distribution (ϕ) along the brush height modelled considering finite EV interactions of varying magnitude (quantified by different values of ν and a given value of ω) and no EV interactions (i.e., $\nu = \omega = 0$). This latter case is exactly identical to the predictions by Zhulina et al. [13]. Smaller H_0 for the case where EV effects have been neglected ensure a denser monomer concentration near to the wall, and accordingly,

driven by the need to ensure a constant N , a smaller monomer concentration away from the wall. Deviation of the brush height due to the consideration of the EV interactions is maximum for larger c_∞ and smaller pH_∞ [see Fig. 2(b)]. Accordingly, for such $c_\infty - pH_\infty$ combinations, the variation in ϕ with and without the EV effects is maximum. Therefore this variation in ϕ between the cases of with and without the EV effects is witnessed to the largest extent in Fig. 3(d) ($c_\infty = 0.1 M$ and $pH_\infty = 3$) and to the least extent in Fig. 3(a) ($c_\infty = 0.01 M$ and $pH_\infty = 4$).

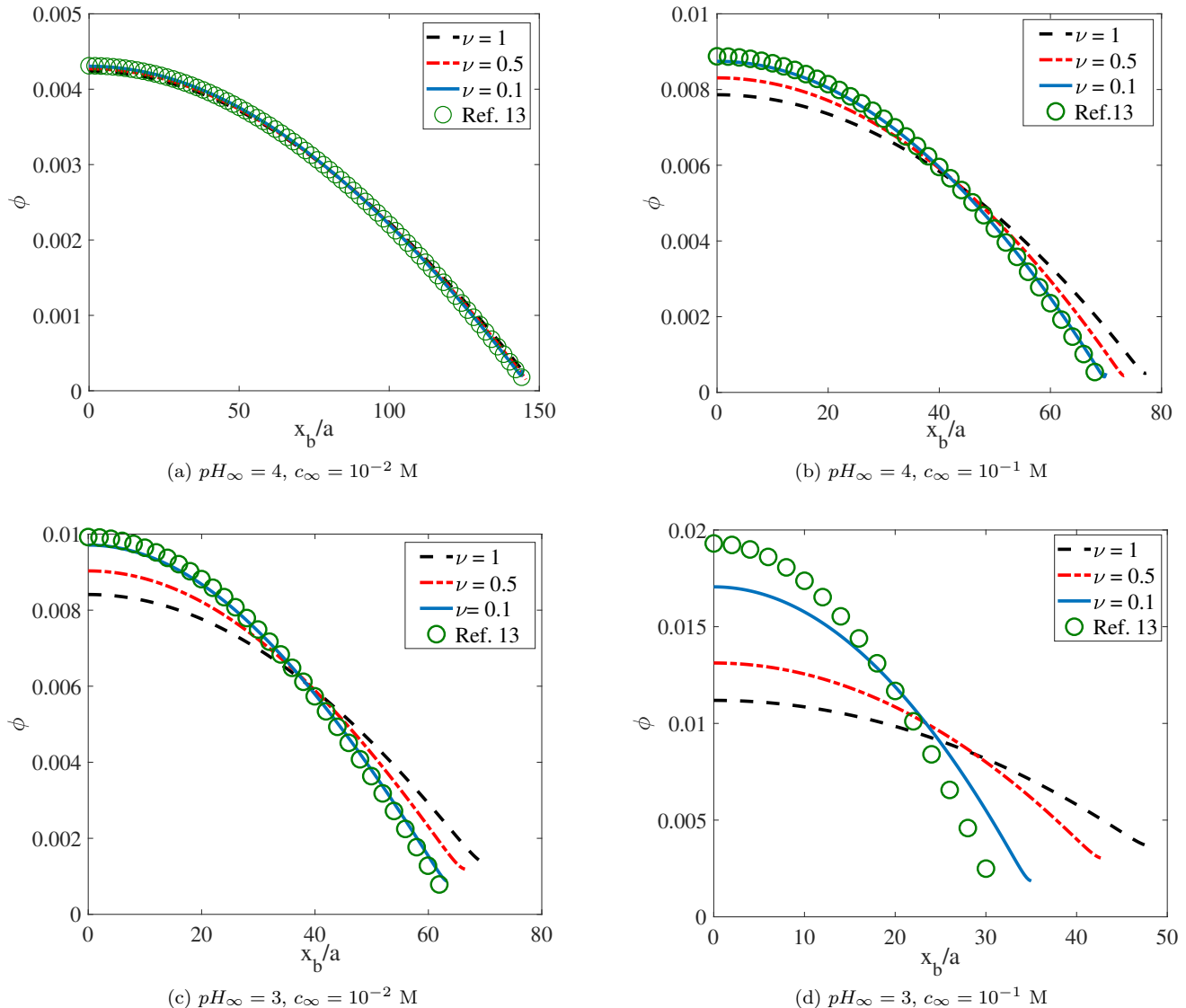


FIG. 3: Comparison of monomer distribution profiles (ϕ) as a function of the dimensionless transverse distance along the brush (x_b/a , a is the Kuhn length) obtained for different values of the first virial coefficient ν using our theory and theory of [13] for different pH_∞ and c_∞ values. All other parameters are identical to that used in Fig. 2.

Fig. 4 provides the variation of the end distribution g of the PE brushes considering finite EV interactions of varying magnitude (quantified by different values of ν and a given value of ω) and no EV interactions (i.e., $\nu = \omega = 0$; this case is that of Ref. [13]). Given that the case without the EV effects lead to a larger concentration of the monomers at near-wall locations, we witness a larger value of g at such near wall locations for the case without the EV effects. On the other hand, an increase in the EV effects, leading to a flatter distribution of ϕ (see Fig. 3), ensures a larger g value much away from the wall. Very much like Figs. 2 and 3, here too the maximum difference between the cases of with and without the EV interactions is witnessed for the condition of large c_∞ and small pH_∞ .

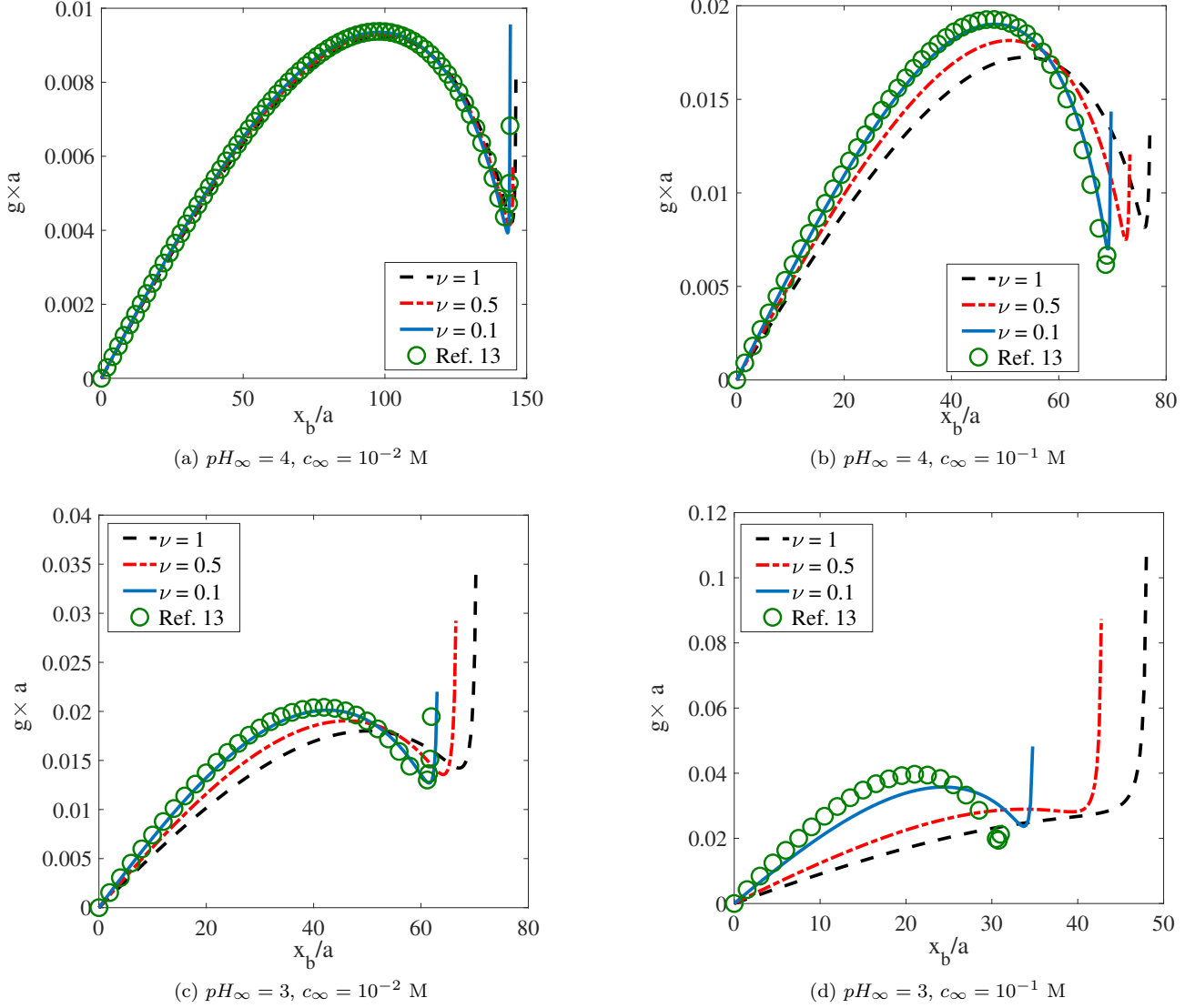


FIG. 4: Comparison of non-dimensional chain end distribution profiles ($g \times a$, a is the Kuhn length) as a function of the dimensionless transverse distance along the brush (x_b/a) obtained for different values of the first virial coefficient ν using our theory and theory of [13] for different pH_∞ and c_∞ values. All other parameters are identical to that used in Fig. 2.

Fig. 5 provides the transverse variation of the EDL electrostatic potential considering both finite EV interactions of varying magnitude between the PE brush segments (quantified by different values of ν and a given value of ω) as well as no EV interactions (i.e., $\nu = \omega = 0$; this case is that of Ref. [13]). The case of no EV interactions correspond to a shorter height of the brush implying a larger per unit volume charge density of the monomers, which in turn would ensure a larger magnitude of the EDL electrostatic potential at near-wall locations. At the same time, the presence of the shorter brushes imply that the brushes extend to smaller distances away from the grafting wall. Accordingly, there is no longer any charge from the brush at some finite distance away from the wall. These two factors simultaneously ensure that the electrostatic potential at near-wall locations is much larger and steeper for the case without the EV effects. The consideration of the EV effects makes the electrostatic potential much smaller and flatter. Here too this difference between the cases that consider or neglect the EV interactions is primarily manifested for large c_∞ and small pH_∞ .

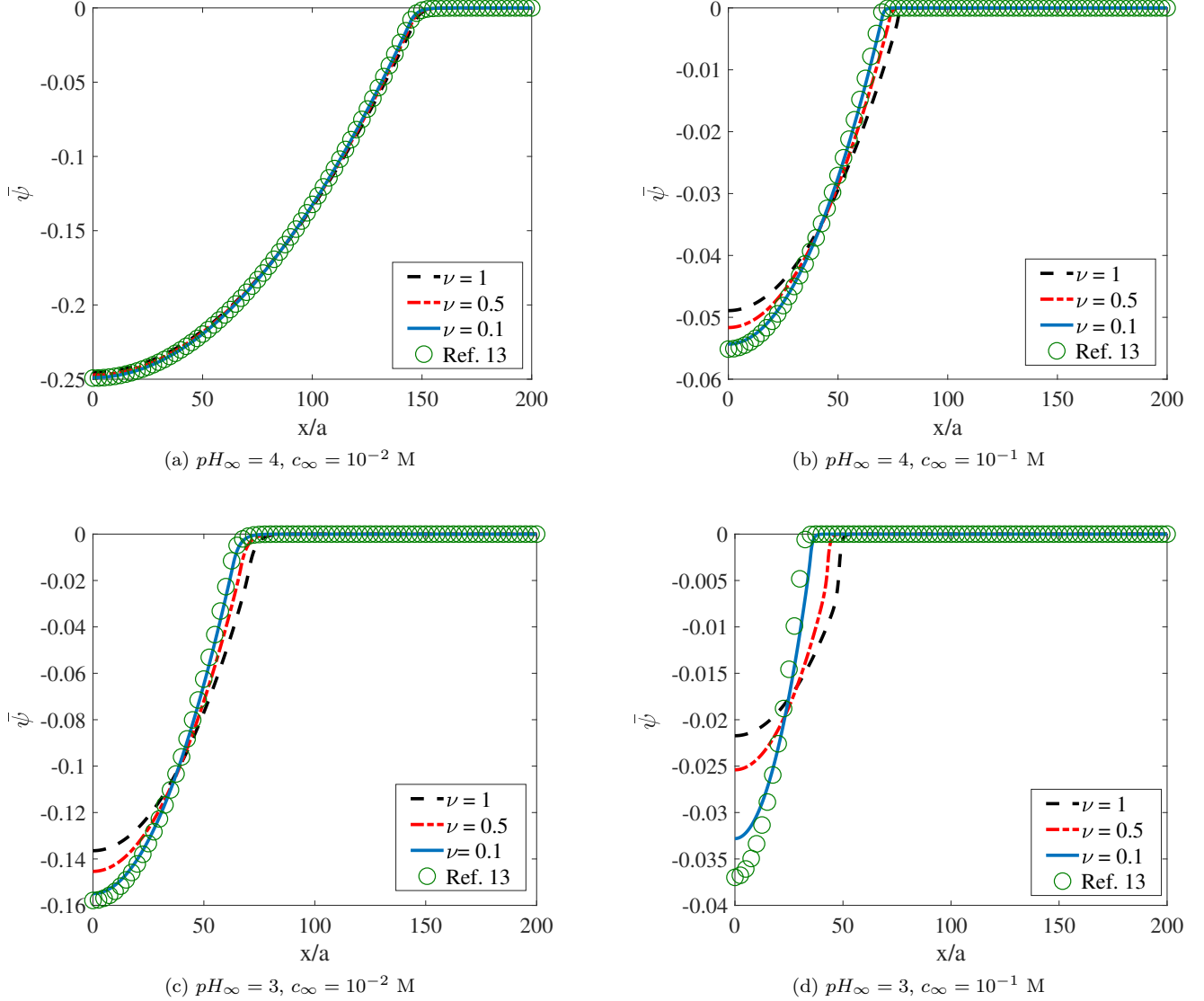


FIG. 5: Comparison of non-dimensional electrostatic potential profiles ($\bar{\psi} = e\psi/(k_B T)$) as a function of the dimensionless transverse distance along the nanochannel half height (x/a) obtained for different values of the first virial coefficient ν using our theory and theory of [13] for different pH_∞ and c_∞ values. All other parameters are identical to that used in Fig. 2.

B. Effects of consideration of an expanded form of the mass action law

We have discussed previously that eq.(16) represents the expanded form of the mass action law and not eq.(21), which has been invariably used in most of the existing studies, but is only a special case of the expanded form of the mass action law obtain for the specific condition of $\gamma = 1/a^3$. In this subsection, we provide results dictating the PE brush configuration and the resultant EDL electrostatics for different values of γ , i.e., study the effect of the consideration of the expanded form of the mass action law. Fig. 6 shows the variation of the equilibrium brush height as a function of γa^3 . Increase in γ or γa^3 implies that the PE molecules has a larger backbone charge density. As a consequence, a larger number of counterions will get localized within the brush in order to screen the larger magnitude of the PE charge. This, in turn, will lead to a larger counterion-induced osmotic swelling of the brushes (reflecting the tendency of the counterions to maximize their entropy by increasing the brush volume), eventually leading to a larger brush height [52–54]. Also, here too, the lowering of the salt concentration (i.e., increasing the EDL thickness, which in turn would lead to a screening of the PE backbone charge over a larger length) and an increase in the pH_∞ (leading to a larger ionization and hence a greater charging of the PE molecule inducing a larger counterion-induced osmotic

swelling) will cause an increase of the PE brush height. Here we also account for the EV interactions quantified by $\nu = 0.1$ and $\omega = 0.01$.

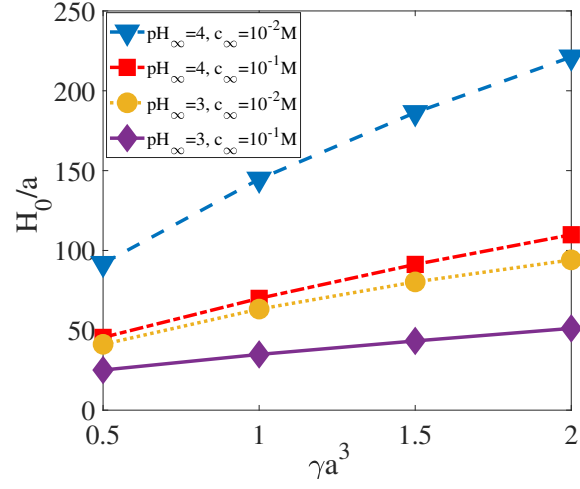


FIG. 6: Variation of non-dimensional equilibrium brush height H_0/a with number of PCS per kuhn monomer γa^3 for different pH_{∞} and c_{∞} values. $\nu = 0.1$, $\omega = 0.01$. All other parameters are identical to that used in Fig. 2.

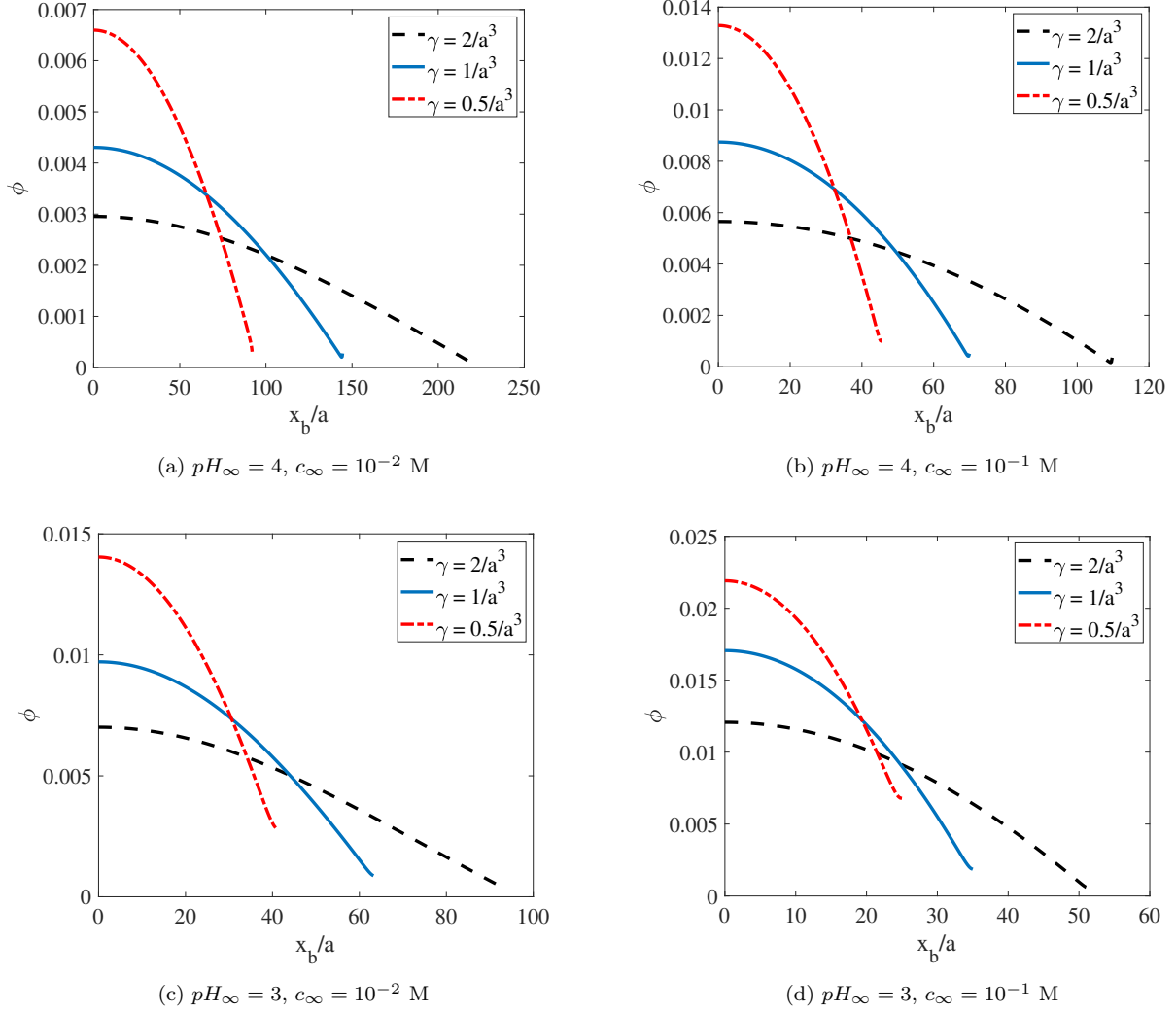


FIG. 7: Comparison of monomer distribution profiles (ϕ) as a function of the dimensionless transverse distance along the brush (x_b/a , a is the Kuhn length) obtained for different values of PCS number density γ using our theory and theory of [13] for different pH_∞ and c_∞ values. $\nu = 0.1$, $\omega = 0.01$. All other parameters are identical to that used in Fig. 2.

Fig. 7 provides the variation of the monomer density along the brush height for different values of γ . It was discussed Fig. 3, a shorter brush would imply a larger (smaller) monomer density close to (away from) the wall in comparison to the cases with larger brush height. This is also the case here – hence we witness a larger (smaller) monomer density close to (away from) the wall for smaller γ values as well as the cases for larger salt concentration and smaller pH_∞ values.

Fig. 8 provides the variation of the end distribution g along the brush height for different values of γ . It was revealed in Fig. 4 that the case of smaller brush height leads to a larger concentration of the monomers close to the wall and results in a larger value of g close to the wall and it decays quickly away from the wall. On the other hand, for the case of larger brush height, g is much smaller at near wall locations and decays much more slowly away from the wall. This is the case here as well – hence we witness a larger (at near wall locations) and a steeply decaying g for the case with small γ (i.e., the case that corresponds to smaller brush height, see Fig. 5), but a smaller and more weakly decaying g for larger γ (i.e., the condition that leads to taller brushes).

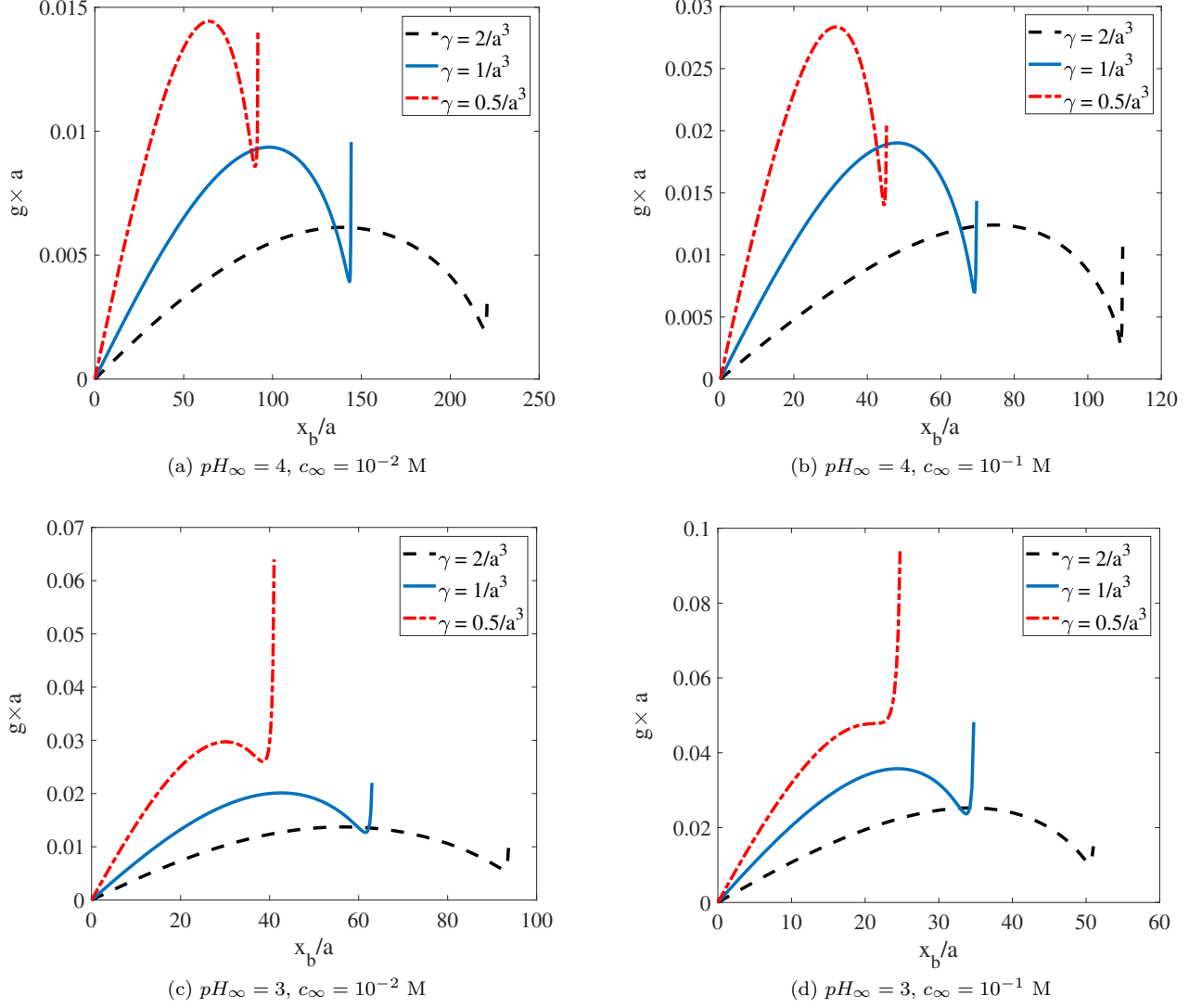


FIG. 8: Comparison of non-dimensional chain end distribution profiles ($g \times a$, a is the Kuhn length) as a function of the dimensionless transverse distance along the brush (x_b/a) obtained for different values of PCS number density γ using our theory and theory of [13] for different pH_∞ and c_∞ values. $\nu = 0.1$, $\omega = 0.01$. All other parameters are identical to that used in Fig. 2.

Finally, Fig. 9 provides the transverse variation of the EDL electrostatic potential for different values of γ . Smaller γ implies both weakened charge density of the brushes as well as shorter brushes. Accordingly, for smaller γ , the EDL electrostatic potential is also weak and also decays quickly (since the brush height is small). Of course, for a given γ , a larger EDL electrostatic potential (magnitude) is invariably witnessed for lower c_∞ (weakened screening of the charge of the PE brushes) and larger pH_∞ (more enhanced ionization of the PE brushes).

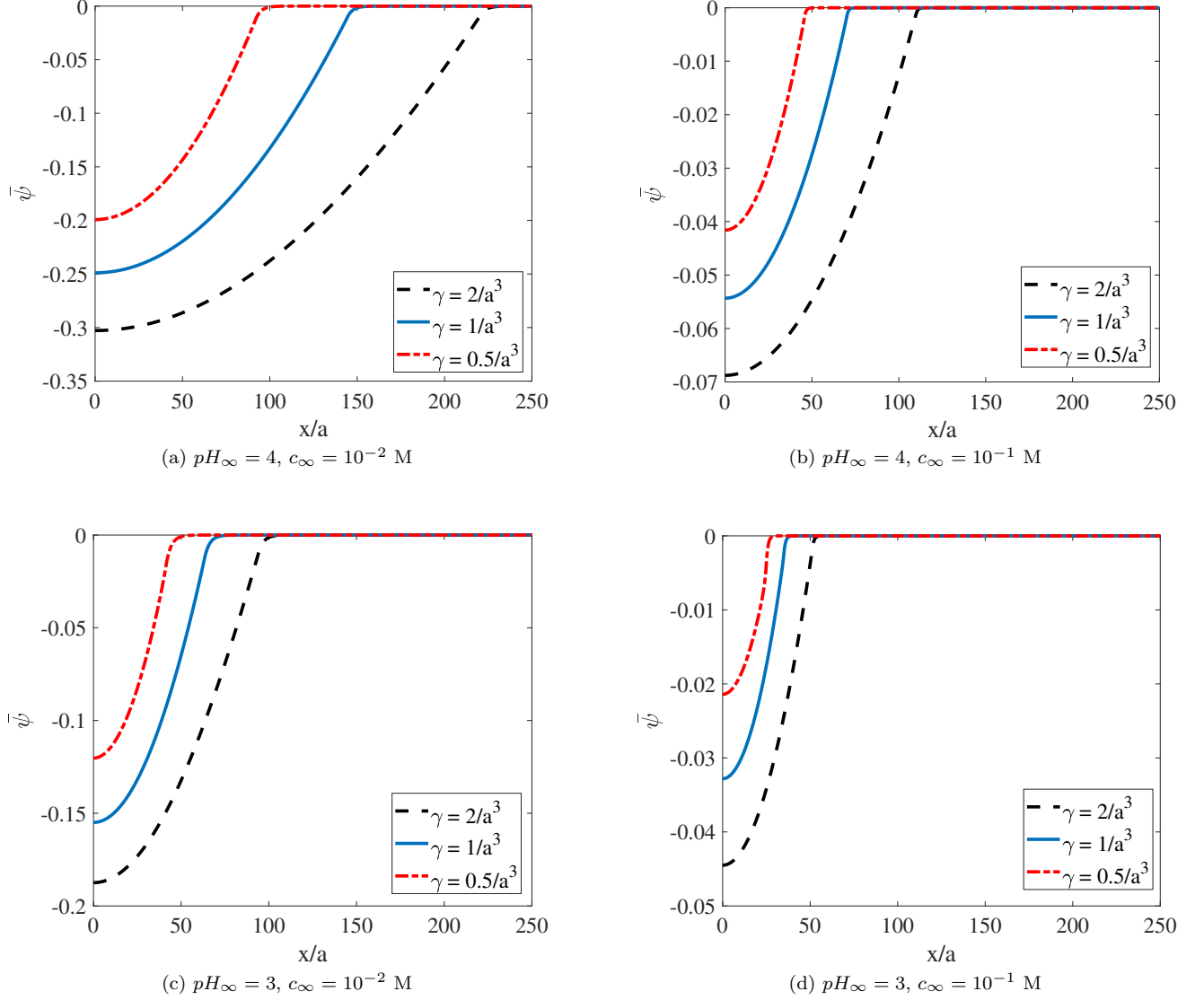


FIG. 9: Comparison of non-dimensional electrostatic potential profiles ($\bar{\psi} = e\psi/(k_B T)$) as a function of the dimensionless transverse distance along the nanochannel half height (x/a) obtained for different values of PCS number density γ using our theory and theory of [13] for different pH_∞ and c_∞ values. $\nu = 0.1$, $\omega = 0.01$. All other parameters are identical to that used in Fig. 2.

IV. DISCUSSIONS

A. Applicability of the Proposed Theory

The proposed theory is directly applicable to all the systems that involve planar, pH-responsive PE brushes. Such brushes have been extensively employed for several applications such as nanochannel ion selectivity [55] and ion detection [56], fabrication of ionic valves [57, 58], nanofluidic diodes [59], and surfaces of controllable wetting properties [60], and many more. The theory provides a new prediction of the EDL electrostatic potential distribution and consequently a new prediction for the number density distribution of the electrolyte, hydrogen, and hydroxyl ions for cases where the EV interactions between the PE segments become important and the PE brushes are so charged that $\gamma a^3 \neq 1$. This would imply that the corresponding changes in the ionic current or the current-voltage characteristics (in presence of an applied voltage), which in turn would dictate several of these applications [55–59], would be significantly different as compared to that obtained with the existing theory [13]. Similarly, the prediction of

a new monomer distribution would critically affect the drag and the resulting fluid flow in brush-grafted nanochannels, which would impact the problems dictated by such fluid flows in brush-grafted nanochannels [14, 16, 61].

The present model, while describes the planar brushes, would also motivate developing models that account for the appropriate EV interactions and the expanded form of the mass action law for the pH-responsive spherical [62] or cylindrical PE brushes (i.e., PE brushes grafted to spheres and cylinders) that have been employed in many applications such as the use of nanoparticles grafted with pH-responsive brushes for targeted drug delivery [63], protein binding [64], synthesis of magnetic nanoparticles [65], etc. Finally, the use of the generic mass action law would be useful to improve the theoretical predictions of not only the pH-responsive planar and curved PE brushes, but also all those calculations that involve generic pH-responsive PE molecules and gels [47–51].

B. Limitations and Scope of Improvement of the Proposed Theory

In this paper, we employ the strong stretching theory (SST) framework which assumes the brushes to be in a strongly stretched configuration. Hence we ignore the effects of lateral variation of monomer distribution profile and bending back of chain ends. The approximation holds good for systems with high grafting density. For other systems, an advanced numerical self-consistent field theory (SCFT) model [66] needs to be implemented.

The second important issue is that we invariably assume that the EDLs are always thin enough to ensure that $\ell \gg 2\lambda_D$ (ℓ is the distance between the adjacent grafted chains and λ_D is the EDL thickness) and there is no overlap between the EDLs formed by the adjacent brushes. In case such an approximation does not hold, one would need to assume a 2D (and not a 1D) model for the brush EDL electrostatics and alter the SST accordingly [67].

Thirdly, no non-PB component (e.g. finite ion size effect [68, 69], solvent polarization effect [70], or ion-ion correlation effect [71]) has been considered in the description of the EDL. These effects would become important for large ψ and large salt concentration and would significantly impact the overall self-consistent field approach.

Fourthly, our theory also does not consider the correlations due to the connectivity of the polymer charges. Such correlations can be specially significant for pH-responsive systems (like pH-responsive PE brushes). For example, there are chances that the effective pK_a of the polymer chain might get significantly altered due to the connected charges of the pH-responsive PE chain [72]. Such alteration of the pK_a and its resulting connotations in all the presented results have been obviously neglected in the present study.

Finally, we shall like to emphasize that given the fact that we have used mean-field calculations in this paper, the capability of the present model to quantify the exact influence of the EV effects will be limited. This stems from the fact that the mean field assumptions extend to the EV effect consideration as well. This has been described in detail by Alexander-Katz et al. [73]. In this paper [73], the authors studied confined polymer solutions and used the density profiles to obtain the effective correlation length ξ_{eff} quantifying the non-mean-field polymer correlations and obtained the results to the mean field theory predictions. While for small EV parameters, the ξ_{eff} was well described by the mean-field theory results, for larger EV parameters $\xi_{eff} \sim C^{-3/4}$ (C is the polymer solution concentration), a result that the mean-field theory could not predict. In essence, therefore, chances are that the inherently mean-field approach of the our calculations would imply that some of the predictions of the effect of considering the EV interactions will be limited.

V. CONCLUSIONS

In this paper, we develop a self-consistent field approach (modified SST) to probe the behavior of the pH-responsive brush system by accounting for (a) the EV interactions between the PE segments and (b) a more expanded form of the mass action law valid for $\gamma a^3 \neq 1$. Results indicate an enhancement of the brush height due to the consideration of the EV interaction driven PE inter-segmental repulsion and an increase (decrease) of the brush height for $\gamma a^3 > 1$ ($\gamma a^3 < 1$) due to increased (decreased) counterion-induced osmotic swelling of the brushes. We also establish that these typical height variations get reflected in the corresponding variations of the monomer density profile, distributions of the PE brush ends, and the corresponding EDL electrostatic potential distribution. This model, which can be considered as the most generic SST model for the pH-responsive PE brushes, will not only be critical for explaining several experiments that invariably consider the PE brushes to be in a “good” solvent, but will also help to better interpret a large number of problems that involve pH-responsive PE molecules (not necessarily in a “brush” configuration) and gels and where a more expanded form of the mass action law with $\gamma a^3 \neq 1$ may be more applicable.

Acknowledgement: This work has been supported by the Department of Energy Office of Science grant DE-SC0017741.

Appendix A: Derivation of eqs.(14-20)

We employ variational calculus to carry out the minimization of the free energy functional [eq.(12)]. Assuming that the chain is flexible ($p=1$) and taking the variation of each free energy component w.r.t. $E(x, x')$, $g(x')$, ψ , n_{A^-} , n_{\pm} , n_{H^+} and n_{OH^-} , we shall get:

$$\begin{aligned} \frac{\delta F'_{els}}{k_B T} = & \frac{3}{2a^2} \left[\int_0^H g(x') dx' \int_0^{x'} \delta E(x, x') dx + \int_0^H \delta g(x') dx' \int_0^{x'} E(x, x') dx \right] + \lambda_1 \frac{\sigma}{a^3} \int_0^H \delta \phi(x) dx \\ & - \int_0^H \lambda_2(x') dx' \int_0^{x'} \frac{\delta E(x, x')}{E^2(x, x')} dx \end{aligned} \quad (A1)$$

$$\frac{\delta F_{EV}}{k_B T} = \frac{\sigma}{a^3} \int_0^H \left(\frac{\delta f_{conc}}{\delta \phi} \right) \delta \phi dx \quad (A2)$$

$$\begin{aligned} \frac{\delta F_{elec}}{k_B T} + \frac{\delta F_{EDL}}{k_B T} = & \frac{\sigma}{k_B T} \int_0^\infty \left[-\frac{\epsilon_0 \epsilon_r}{2} \delta \left| \frac{d\psi}{dx} \right|^2 + e \delta \psi (n_+ - n_- + n_{H^+} - n_{OH^-}) + e \psi (\delta n_+ - \delta n_- + \delta n_{H^+} - \delta n_{OH^-}) \right] dx \\ & - \frac{\sigma}{k_B T} \int_0^H \delta \left[e \psi n_{A^-}(x) \phi \right] dx + \sigma \int_0^\infty \delta \left[n_+ \left(\ln \left(\frac{n_+}{n_{+, \infty}} \right) - 1 \right) + n_- \left(\ln \left(\frac{n_-}{n_{-, \infty}} \right) - 1 \right) \right. \\ & \left. + n_{H^+} \left(\ln \left(\frac{n_{H^+}}{n_{H^+, \infty}} \right) - 1 \right) + n_{OH^-} \left(\ln \left(\frac{n_{OH^-}}{n_{OH^-, \infty}} \right) - 1 \right) + (n_{+, \infty} + n_{-, \infty} + n_{H^+, \infty} + n_{OH^-, \infty}) \right] dx \\ = & \frac{\sigma}{k_B T} \int_0^\infty \left[\epsilon_0 \epsilon_r \left(\frac{d^2 \psi}{dx^2} \right) \delta \psi + e \delta \psi (n_+ - n_- + n_{H^+} - n_{OH^-}) + e \psi (\delta n_+ - \delta n_- + \delta n_{H^+} - \delta n_{OH^-}) \right] dx \\ & - \frac{\sigma}{k_B T} \int_0^H \left[e \phi \left(\frac{K'_a \gamma}{K'_a + n_{H^+}} \right) \delta \psi - e \phi \psi \frac{K'_a \gamma}{(K'_a + n_{H^+})^2} \delta n_{H^+} + e \psi \left(\frac{K'_a \gamma}{K'_a + n_{H^+}} \right) \delta \phi \right] dx \\ & + \sigma \int_0^\infty \left[\delta n_+ \ln \left(\frac{n_+}{n_{+, \infty}} \right) + \delta n_- \ln \left(\frac{n_-}{n_{-, \infty}} \right) + \delta n_{H^+} \ln \left(\frac{n_{H^+}}{n_{H^+, \infty}} \right) + \delta n_{OH^-} \ln \left(\frac{n_{OH^-}}{n_{OH^-, \infty}} \right) \right] dx \end{aligned} \quad (A3)$$

$$\begin{aligned} \frac{\delta F_{ion}}{k_B T} = & \frac{\sigma}{a^3} \int_0^H \delta \phi \left[\left(1 - \frac{n_{A^-}}{\gamma} \right) \ln \left(1 - \frac{n_{A^-}}{\gamma} \right) + \frac{n_{A^-}}{\gamma} \ln \left(\frac{n_{A^-}}{\gamma} \right) + \frac{n_{A^-}}{\gamma} \ln \left(\frac{n_{H^+, \infty}}{K'_a} \right) \right] dx \\ & + \frac{\sigma}{a^3} \int_0^H \phi \delta \left[\left(1 - \frac{n_{A^-}}{\gamma} \right) \ln \left(1 - \frac{n_{A^-}}{\gamma} \right) + \frac{n_{A^-}}{\gamma} \ln \left(\frac{n_{A^-}}{\gamma} \right) + \frac{n_{A^-}}{\gamma} \ln \left(\frac{n_{H^+, \infty}}{K'_a} \right) \right] dx \\ = & \frac{\sigma}{a^3} \int_0^H \delta \phi \left[\left(1 - \frac{n_{A^-}}{\gamma} \right) \ln \left(1 - \frac{n_{A^-}}{\gamma} \right) + \frac{n_{A^-}}{\gamma} \ln \left(\frac{n_{A^-}}{\gamma} \right) + \frac{n_{A^-}}{\gamma} \ln \left(\frac{n_{H^+, \infty}}{K'_a} \right) \right] \\ & + \frac{\sigma}{a^3} \int_0^H \phi \delta n_{A^-} \left[-\frac{1}{\gamma} \ln \left(1 - \frac{n_{A^-}}{\gamma} \right) + \frac{1}{\gamma} \ln \left(\frac{n_{A^-}}{\gamma} \right) + \frac{1}{\gamma} \ln \left(\frac{n_{H^+, \infty}}{K'_a} \right) \right] dx \end{aligned} \quad (A4)$$

Substituting eq.(A1), (A2), (A3) and (A4) in (13), we get:

$$\begin{aligned}
\frac{\delta F'}{k_B T} = & \frac{3}{2pa^2} \left[\int_0^H g(x') dx' \int_0^{x'} \delta E(x, x') dx + \int_0^H \delta g(x') dx' \int_0^{x'} E(x, x') dx \right] + \lambda_1 \frac{\sigma}{a^3} \int_0^H \delta \phi(x) dx \\
& - \int_0^H \lambda_2(x') dx' \int_0^{x'} \frac{\delta E(x, x')}{E^2(x, x')} dx + \frac{\sigma}{a^3} \int_0^H \left(\frac{\delta f_{conc}}{\delta \phi} \right) \delta \phi dx \\
& + \frac{\sigma}{k_B T} \int_0^\infty \left[\epsilon_0 \epsilon_r \left(\frac{d^2 \psi}{dx^2} \right) \delta \psi + e \delta \psi (n_+ - n_- + n_{H^+} - n_{OH^-}) + e \psi (\delta n_+ - \delta n_- + \delta n_{H^+} - \delta n_{OH^-}) \right] dx \\
& - \frac{\sigma}{k_B T} \int_0^H \left[e \phi n_{A^-} \delta \psi + e \phi \psi \delta n_{A^-} + e \psi n_{A^-} \delta \phi \right] dx \\
& + \sigma \int_0^\infty \left[\delta n_+ \ln \left(\frac{n_+}{n_{+, \infty}} \right) + \delta n_- \ln \left(\frac{n_-}{n_{-, \infty}} \right) + \delta n_{H^+} \ln \left(\frac{n_{H^+}}{n_{H^+, \infty}} \right) + \delta n_{OH^-} \ln \left(\frac{n_{OH^-}}{n_{OH^-, \infty}} \right) \right] dx \\
& + \frac{\sigma}{a^3} \int_0^H \delta \phi \left[\left(1 - \frac{n_{A^-}}{\gamma} \right) \ln \left(1 - \frac{n_{A^-}}{\gamma} \right) + \frac{n_{A^-}}{\gamma} \ln \left(\frac{n_{A^-}}{\gamma} \right) + \frac{n_{A^-}}{\gamma} \ln \left(\frac{n_{H^+, \infty}}{K'_a} \right) \right] dx \\
& + \frac{\sigma}{a^3} \int_0^H \delta n_{A^-} \phi \left[-\frac{1}{\gamma} \ln \left(1 - \frac{n_{A^-}}{\gamma} \right) + \frac{1}{\gamma} \ln \left(\frac{n_{A^-}}{\gamma} \right) + \frac{1}{\gamma} \ln \left(\frac{n_{H^+, \infty}}{K'_a} \right) \right] dx
\end{aligned} \tag{A5}$$

Variation of eq.(10) gives:

$$\delta \phi(x) = \frac{a^3}{\sigma} \int_x^H \left[\frac{\delta g(x')}{E(x, x')} - \frac{g(x') \delta E(x, x')}{E^2(x, x')} \right] dx' \tag{A6}$$

Substituting eq.(A6) in (A5) and rearranging gives:

$$\begin{aligned}
\frac{\delta F'}{k_B T} = & \int_0^H dx' \int_0^{x'} \delta E(x, x') \left[\frac{3g(x')}{2pa^2} - \frac{\lambda_2(x')}{E^2(x, x')} - \left(\frac{\delta f_{conc}}{\delta \phi} + \lambda_1 - \frac{ea^3 \psi}{k_B T} n_{A^-} + \left(1 - \frac{n_{A^-}}{\gamma} \right) \ln \left(1 - \frac{n_{A^-}}{\gamma} \right) \right. \right. \\
& \left. \left. + \frac{n_{A^-}}{\gamma} \ln \left(\frac{n_{A^-}}{\gamma} \right) + \frac{n_{A^-}}{\gamma} \ln \left(\frac{n_{H^+, \infty}}{K'_a} \right) \right) \frac{g(x')}{E^2(x, x')} \right] dx \\
& + \int_0^H dx' \delta g(x') \int_0^{x'} \left[\frac{3E(x, x')}{2pa^2} + \left(\frac{\delta f_{conc}}{\delta \phi} + \lambda_1 - \frac{ea^3 \psi}{k_B T} n_{A^-} + \left(1 - \frac{n_{A^-}}{\gamma} \right) \ln \left(1 - \frac{n_{A^-}}{\gamma} \right) + \frac{n_{A^-}}{\gamma} \ln \left(\frac{n_{A^-}}{\gamma} \right) \right. \right. \\
& \left. \left. + \frac{n_{A^-}}{\gamma} \ln \left(\frac{n_{H^+, \infty}}{K'_a} \right) \right) \frac{1}{E(x, x')} \right] dx \\
& + \frac{\sigma}{\gamma a^3} \int_0^H \delta n_{A^-} \phi \left[-\gamma a^3 \frac{e \psi}{k_B T} - \ln \left(1 - \frac{n_{A^-}}{\gamma} \right) + \ln \left(\frac{n_{A^-}}{\gamma} \right) + \ln \left(\frac{n_{H^+, \infty}}{K'_a} \right) \right] dx \\
& + \frac{\sigma}{k_B T} \int_0^H \delta \psi \left[\epsilon_0 \epsilon_r \left(\frac{d^2 \psi}{dx^2} \right) + e \left(n_+ - n_- + n_{H^+} - n_{OH^-} - n_{A^-} \phi \right) \right] dx \\
& + \frac{\sigma}{k_B T} \int_H^\infty \delta \psi \left[\epsilon_0 \epsilon_r \left(\frac{d^2 \psi}{dx^2} \right) + e \left(n_+ - n_- + n_{H^+} - n_{OH^-} \right) \right] dx + \sigma \int_0^\infty \delta n_+ \left[\frac{e \psi}{k_B T} + \ln \left(\frac{n_+}{n_{+, \infty}} \right) \right] dx \\
& + \sigma \int_0^\infty \delta n_- \left[-\frac{e \psi}{k_B T} + \ln \left(\frac{n_-}{n_{-, \infty}} \right) \right] dx + \sigma \int_0^\infty \delta n_{H^+} \left[\frac{e \psi}{k_B T} + \ln \left(\frac{n_{H^+}}{n_{H^+, \infty}} \right) \right] dx \\
& + \sigma \int_0^\infty \delta n_{OH^-} \left[-\frac{e \psi}{k_B T} + \ln \left(\frac{n_{OH^-}}{n_{OH^-, \infty}} \right) \right] dx
\end{aligned} \tag{A7}$$

Equating $\delta F' = 0$ yields the desired eqs.(14-20) since $\delta E(x, x') \neq 0$, $\delta g(x') \neq 0$, $\delta \psi \neq 0$, $\delta n_{A^-} \neq 0$, $\delta n_{\pm} \neq 0$, $\delta n_{H^+} \neq 0$, $\delta n_{OH^-} \neq 0$.

-
- [1] de Groot, G. W.; Santonicola, M. G.; Sugihara, K.; Zambelli, T.; Reimhult, E.; Voros, J.; Vancso, G. J. Switching Transport through Nanopores with pH-Responsive Polymer Brushes for Controlled Ion Permeability. *ACS Appl. Mater. Interface.* **2013**, *5*, 1400–1407.
- [2] Yameen, B.; Ali, M.; Neumann, R.; Ensinger, W.; Knoll, W.; Azzaroni, O. Single Conical Nanopores Displaying pH-Tunable Rectifying Characteristics. Manipulating Ionic Transport with Zwitterionic Polymer Brushes. *J. Am. Chem. Soc.* **2009**, *131*, 2070–2071.
- [3] Ali, M.; Yameen, B.; Neumann, R.; Ensinger, W.; Knoll, W.; Azzaroni, O. Biosensing and Supramolecular Bioconjugation in Single Conical Polymer Nanochannels. Facile Incorporation of Biorecognition Elements into Nanoconfined Geometries. *J. Am. Chem. Soc.*, **2008**, *130*, 16351–16357.
- [4] Ali, M.; Schiedt, B.; Neumann, R.; Ensinger, W. Biosensing with Functionalized Single Asymmetric Polymer Nanochannels. *Macromol. Biosci.* **2010**, *10*, 28–32.
- [5] Umehara, S.; Karhanek, M.; Davis, R. W.; Pourmand, N. Label-Free Biosensing with Functionalized Nanopipette Probes. *Proc. Natl. Acad. Sci.* **2009**, *106*, 4611–4616.
- [6] Viložny, B.; Wollenberg, A. L.; Actis, P.; Hwang, D.; Singaram, B.; Pourmand, N. Carbohydrate-Actuated Nanofluidic Diode: Switchable Current Rectification in a Nanopipette. *Nanoscale* **2013**, *5*, 9214–9221.
- [7] Ali, M.; Ramirez, P.; Mafe, S.; Neumann, R.; Ensinger, W. A pH-Tunable Nanofluidic Diode with a Broad Range of Rectifying Properties. *ACS Nano* **2009**, *3*, 603–608.
- [8] Ali, M.; Yameen, B.; Cervera, J.; Ramirez, P.; Neumann, R.; Ensinger, W.; Knoll, W.; Azzaroni, O. Layer-By-Layer Assembly of Polyelectrolytes into Ionic Current Rectifying Solid-State Nanopores: Insights from Theory and Experiment. *J. Am. Chem. Soc.* **2010**, *132*, 8338–8348.
- [9] Moya, S.; Azzaroni, O.; Farhan, T.; Osborne, V. L.; Huck, W. T. S. Locking and Unlocking of Polyelectrolyte Brushes: Toward the Fabrication of Chemically Controlled Nanoactuators. *Angewand. Chem. Int. Ed.* **2005**, *44*, 4578–4581.
- [10] Xin, B.; Hao, J. Reversibly Switchable Wettability. *Chem. Soc. Rev.* **2010**, *39*, 769–782.
- [11] Mura, S.; Nicolas, J.; Couvreur, P. Stimuli-Responsive Nanocarriers for Drug Delivery. *Nature Mater.* **2013**, *12*, 991.
- [12] ShamsiJazeyi, H.; Miller, C. A.; Wong, J. S.; Tour, J. M.; Verduzco, R. Polymer-Coated Nanoparticles for Enhanced Oil Recovery. *J. Appl. Pol. Sci.* **2014**, *131*, 40576.
- [13] Zhulina, E. B.; Borisov, O. V. Poisson–Boltzmann Theory of pH-Sensitive (Annealing) Polyelectrolyte Brush. *Langmuir* **2011**, *27*, 10615–10633.
- [14] Patwary, J.; Chen, G.; Das, S. Efficient Electrochemomechanical Energy Conversion in Nanochannels Grafted with Polyelectrolyte Layers with pH-Dependent Charge Density. *Microfluid. Nanofluid.* **2016**, *20*, 37.
- [15] Chen, G.; Das, S. Scaling Laws and Ionic Current Inversion in Polyelectrolyte-Grafted Nanochannels. *J. Phys. Chem. B* **2015**, *119*, 12714–12726.
- [16] Chen, G.; Das, S. Electroosmotic Transport in Polyelectrolyte-Grafted Nanochannels with pH-Dependent Charge Density. *J. Appl. Phys.* **2015**, *117*, 185304.
- [17] Chen, G.; Das, S. Electrostatics of Soft Charged Interfaces with pH-Dependent Charge Density: Effect of Consideration of Appropriate Hydrogen Ion Concentration Distribution. *RSC Adv.* **2015**, *5*, 4493–4501.
- [18] Pincus, P. A. Colloid Stabilization with Grafted Polyelectrolytes. *Macromolecules* **1991**, *24*, 2912–2919.
- [19] Ross, R.; Pincus, P. A. The polyelectrolyte brush: poor solvent. *Macromolecules* **1992**, *25*, 2177–2183.
- [20] Borisov, O. V.; Birshtein, T. M.; Zhulina, E. B. Collapse of Grafted Polyelectrolyte layer. *J. Phys. II* **1991**, *1*, 521–526.
- [21] Wittmer, J.; Joanny, J. F. Charged Diblock Copolymers at Interfaces. *Macromolecules* **1993**, *26*, 2691–2697.
- [22] Borisov, O. V.; Zhulina, E. B.; Birshtein, T. M. Diagram of the States of a Grafted Polyelectrolyte Layer. *Macromolecules* **1994**, *27*, 4795–4803.
- [23] Zhulina, E. B.; Birshtein, T. M.; Borisov, O. V. Theory of Ionizable Polymer Brushes. *Macromolecules* **1995**, *28*, 1491–1499.
- [24] Zhulina, E. B.; Rubinstein, M. Ionic Strength Dependence of Polyelectrolyte Brush Thickness. *Soft Matt.* **2012**, *8*, 9376–9383.
- [25] Israëls, R.; Leermakers, F. A. M.; Fleer, G. J.; Zhulina, E. B. Charged Polymeric Brushes: Structure and Scaling Relations. *Macromolecules* **1994**, *27*, 3249–3261.
- [26] Misra, S.; Varanasi, S.; Varanasi, P. P. A Polyelectrolyte Brush Theory. *Macromolecules* **1989**, *22*, 4173–4179.
- [27] Chen, G.; Das, S. Anomalous Shrinking–Swelling of Nanoconfined End-Charged Polyelectrolyte Brushes: Interplay of Confinement and Electrostatic Effects. *J. Phys. Chem. B* **2016**, *120*, 6848–6857.
- [28] Chen, G.; Das, S. Assively Enhanced Electroosmotic Transport in Nanochannels Grafted with End-Charged Polyelectrolyte Brushes. *J. Phys. Chem. B* **2017**, *121*, 3130–3141.
- [29] Chen, G.; Sachar, H. S.; Das, S. Efficient Electrochemomechanical Energy Conversion in Nanochannels Grafted with End-Charged Polyelectrolyte Brushes at Medium and High Salt Concentration. *Soft Matt.* **2018**, *14*, 5246–5255.
- [30] Maheedhara, R. S.; Sachar, H. S.; Jing, H.; Das, S. Ionic Diffusosmosis in Nanochannels Grafted with End-Charged Polyelectrolyte Brushes. *J. Phys. Chem. B*, *122*, 7450–7461.
- [31] Biesheuvel, P. M.; de Vos, W. M.; Amoskov, V. M. Semianalytical Continuum Model for Nondilute Neutral and Charged

Brushes Including Finite Stretching. *Macromolecules* **2008**, *41*, 6254–6259.

- [32] Zhulina, E. B.; Borisov, O. V. Structure and Interaction of Weakly Charged Polyelectrolyte Brushes: Self-Consistent Field Theory. *J. Chem. Phys.* **1997**, *107*, 5952–5967.
- [33] Lyatskaya, Y. V.; Leermakers, F. A. M.; Fleer, G. J.; Zhulina, E. B.; Birshtein, T. M. Analytical Self-Consistent-Field Model of Weak Polyacid Brushes. *Macromolecules* **1995**, *28*, 3562–3569.
- [34] Lebedeva, I. O.; Zhulina, E. B.; Borisov, O. V. Self-Consistent Field Theory of Polyelectrolyte Brushes with Finite Chain Extensibility. *J. Chem. Phys.* **2017**, *146*, 214901.
- [35] Zhulina, E. B.; Wolterink, J. K.; Borisov, O. V. Screening Effects in a Polyelectrolyte Brush: Self-Consistent-Field Theory. *Macromolecules* **2000**, *33*, 4945–4953.
- [36] Mahalik, J. P.; Yang, Y.; Deodhar, C.; Ankner, J. F.; Lokitz, B. S.; Kilbey II, S. M.; Sumpter, B. G.; Kumar, R. Monomer Volume Fraction Profiles in pH Responsive Planar Polyelectrolyte Brushes. *J. Pol. Sci. B* **2016**, *54*, 956–964.
- [37] Wu, T.; Gong, P.; Szeifer, I.; Vlcek, P.; Subr, V.; Genzer, J. Behavior of Surface-Anchored Poly(acrylic acid) Brushes with Grafting Density Gradients on Solid Substrates: 1. Experiment. *Macromolecules* **2007**, *40*, 8756–8764.
- [38] Ito, Y.; Park, Y. S.; Imanishi, Y. Visualization of Critical pH-Controlled Gating of a Porous Membrane Grafted with Polyelectrolyte Brushes. *J. Am. Chem. Soc.* **1997**, *119*, 2739–2740.
- [39] Li, D.; He, Q.; Yang, Y.; Möhwald, H.; Li, J. Two-Stage pH Response of Poly(4-vinylpyridine) Grafted Gold Nanoparticles. *Macromolecules* **2008**, *41*, 7254–7256.
- [40] Wang, M.; Zou, S.; Guerin, G.; Shen, L.; Deng, K.; Jones, M.; Walker, G. C.; Scholes, G. D.; Winnik, M. A. A Water-Soluble pH-Responsive Molecular Brush of Poly(N,N-dimethylaminoethyl methacrylate) Grafted Polythiophene. *Macromolecules* **2008**, *41*, 6993–7002.
- [41] Murdoch, J. T.; Willott, J. D.; de Vos, Nelson, A.; Prescott, S. W.; Wanless, E. J.; Webber, G. B. Influence of Anion Hydrophilicity on the Conformation of a Hydrophobic Weak Polyelectrolyte Brush. *Macromolecules* **2016**, *49*, 9605–9617.
- [42] Cheesman, B. T.; Neilson, A. J. G.; Willott, J. D.; Webber, G. B.; Edmondson, S.; Wanless, E. J. *Langmuir* **2013**, *29*, 6131–6140.
- [43] Willott, J. D.; Murdoch, T. J.; Humphreys, B. A.; Edmondson, S.; Wanless, E. J.; Webber, G. B. Anion-Specific Effects on the Behavior of pH-Sensitive Polybasic Brushes. *Langmuir* **2015**, *31*, 3707–3717.
- [44] Zhulina, E. B.; Pryamitsyn, V. A.; Borisov, O. V. Structure and Conformational Transitions in Grafted Polymer Chain Layers. A New Theory. *Pol. Sci. USSR* **1989**, *31*, 205–216.
- [45] Willott, J. D.; Murdoch, T. J.; Leermakers, F. A. M.; de Vos, W. M. Behavior of Weak Polyelectrolyte Brushes in Mixed Salt Solutions. *Macromolecules* **2018**, *51*, 1198–1206.
- [46] Hariharan, R.; Biver, C.; Russel, W. B. Ionic Strength Effects in Polyelectrolyte Brushes: The Counterion Correction. *Macromolecules* **1998**, *31*, 7514–7518.
- [47] Uline, M. J.; Rabin, Y.; Szeifer, I. Effects of the Salt Concentration on Charge Regulation in Tethered Polyacid Monolayers. *Langmuir* **2011**, *27*, 4679–4689.
- [48] Longo, G. S.; de la Cruz, M. O.; Szeifer, I. Molecular Theory of Weak Polyelectrolyte Gels: The Role of pH and Salt Concentration. *Macromolecules* **2011**, *44*, 147–158.
- [49] Morochnik, S.; Nap, R. J.; Ameer, G. A.; Szeifer, I. Structural Behavior of Competitive Temperature and pH-Responsive Tethered Polymer Layers. *Soft Matt.* **2017**, *13*, 6332–6331.
- [50] Longo, G. S.; Szeifer, I. Adsorption and Protonation of Peptides and Proteins in pH Responsive Gels. *J. Phys. D. Appl. Phys.* **2016**, *49*, 323001.
- [51] Gilles, F. M.; Tagliazucchi, M.; Azzaroni, O.; Szeifer, I. Ionic Conductance of Polyelectrolyte-Modified Nanochannels: Nanoconfinement Effects on the Coupled Protonation Equilibria of Polyprotic Brushes. *J. Phys. Chem. C* **2016**, *120*, 4789–4798.
- [52] Zhulina, E. B.; Rubinstein, M. Lubrication by Polyelectrolyte Brushes. *Macromolecules* **2014**, *47*, 5825–5838.
- [53] Kumar, N. A.; Seidel, C. Polyelectrolyte Brushes with Added Salt. *Macromolecules* **2005**, *38*, 9348–9350.
- [54] Naji, A.; Netz, R. R.; Seidel, C. Non-linear Osmotic Brush Regime: Simulations and Mean-field theory. *Eur. Phys. J. E* **2003**, *12*, 223–237.
- [55] Zeng, Z.; Yeh, L.-H.; Zhang, M.; Qian, S. Ion Transport and Selectivity in Biomimetic Nanopores with pH-Tunable Zwitterionic Polyelectrolyte Brushes. *Nanoscale* **2015**, *7*, 17020–17029.
- [56] Niu, B.; Xiao, K.; Huang, X.; Zhang, Z.; Kong, X.-Y.; Wang, Z.; Wen, L.; Jiang, L. High-Sensitivity Detection of Iron(III) by Dopamine-Modified Funnel-Shaped Nanochannels. *ACS Appl. Mater. Interfaces* **2018**, *10*, 22632–22639.
- [57] Liu, M.; Zhang, H.; Li, K.; Heng, L.; Wang, S.; Tian, Y.; Jian, L. A Bioinspired Potassium and pH Responsive Doublegated Nanochannel. *Adv. Func. Mater.* **2015**, *25*, 421–426.
- [58] Lopez, L. G.; Nap, R. J. Highly Sensitive Gating in pH-Responsive Nanochannels as a Result of Ionic Bridging and Nanoconfinement. *Phys. Chem. Chem. Phys.* **2018**, *20*, 16657–16665.
- [59] Zhang, M.; Hou, X.; Wang, J.; Tian, Y.; Fan, X.; Zhai, J.; Jiang, L. Light and pH Cooperative Nanofluidic Diode using a Spiropyran-Functionalized Single Nanochannel. *Adv. Mater.* **2012**, *24*, 2424–2428.
- [60] Azzaroni, O.; Brown, A. A.; Huck, W. T. S. Tunable Wettability by Clicking Counterions into Polyelectrolyte Brushes. *Adv. Mater.* **2007**, *19*, 151–154.
- [61] Chen, G.; Patwary, J.; Sachar, H. S.; Das, S. Electrokinetics in Nanochannels Grafted with Poly-zwitterionic Brushes. *Microfluid. Nanofluid.* **2018**, *22*, 112.
- [62] Li, H.; Chen, G.; Das, S. Electric Double Layer Electrostatics of pH-Responsive Spherical Polyelectrolyte Brushes in the Decoupled Regime. *Colloid. Surf. B* **2016**, *147*, 180–190.
- [63] Motornov, M.; Tam, T. K.; Pita, M.; Tokarev, I.; Katz, E.; Minko, S. Switchable Selectivity for Gating Ion Transport with

- Mixed Polyelectrolyte Brushes: Approaching SmartDrug Delivery Systems. *Nanotechnology* **2009**, 20, 434006.
- [64] Wang, S.; Chen, K.; Li, L.; Guo, X. Binding between Proteins and Cationic Spherical Polyelectrolyte Brushes: Effect of pH, Ionic strength, and Stoichiometry. *Biomacromolecules* **2013**, 14, 818–827.
- [65] Zhu, Y.; Chen, K.; Wang, X.; Guo, X. Spherical Polyelectrolyte Brushes as a Nanoreactor for Synthesis of Ultrafine Magnetic Nanoparticles. *Nanotechnology* **2012**, 23, 265601.
- [66] Kumar, R.; Sumpter, B. G.; Kilbey, S. M. Charge Regulation and Local Dielectric Function in Planar Polyelectrolyte Brushes. *J. Chem. Phys.* **2012**, 136, 234901.
- [67] Deshkovski, A.; Obukhov, S.; Rubinstein, M. Counterion Phase Transitions in Dilute Polyelectrolyte Solutions. *Phys. Rev. Lett.* **2001**, 86, 2341–2344.
- [68] Kilic, M. S.; Bazant, M. Z.; Ajdari, A. Steric Effects in the Dynamics of Electrolytes at Large Applied Voltages. I. Double-Layer Charging. *Phys. Rev. E* **2007**, 75, 021502.
- [69] Chanda, S.; Das, S. Effect of Finite Ion Sizes in an Electrostatic Potential Distribution for a Charged Soft Surface in Contact with an Electrolyte Solution. *Phys. Rev. E* **2014**, 89, 012307.
- [70] Misra, R. P.; Das, S.; Mitra, S. K. Electric Double Layer Force between Charged Surfaces: Effect of Solvent Polarization. *J. Chem. Phys.* **2013**, 138, 114703.
- [71] Storey, B. D.; Bazant, M. Z. Effects of Electrostatic Correlations on Electrokinetic Phenomena. *Phys. Rev. E* **2012**, 86, 056303.
- [72] Rathee, V. S.; Sikora, B. J.; Sidky, H.; Whitmer, J. K. Simulating the Thermodynamics of Charging in Weak Polyelectrolytes: the Debye-Hückel Limit. *Mater. Res. Exp.* **2018**, 5, 014010.
- [73] Alexander-Katz, A.; Moreira, A. G.; Fredrickson, G. H. Field-theoretic Simulations of Confined Polymer Solutions. *J. Chem. Phys.* **2003**, 118, 9030–9036.